EAI Endorsed Transactions
on Wireless Spectrum

Research Article EAI.EU

On Performance Improvement of Centroid Topology Optimization Schemes in LTE Networks

Jin Zhang[1], Yalong Wu[1], James Nguyen[2], Wei Yu[1,*], Chao Lu[1], and Daniel Ku[2]

[1]Dept. of Computer and Information Sciences, Towson University, Towson, MD USA.
[2]US Army Communications-Electronics Research, Development, and Engineering Center (CERDEC), Aberdeen Proving Ground, MD, USA.

Abstract

In Long Term Evolution (LTE) networks, centroid topology optimization (CTO)-based schemes have been widely used to construct network topologies such that overall network performance is improved. In this paper, we systematically analyze CTO-based schemes and develop new schemes to improve network performance by reconnecting disconnected devices. First, we conduct an investigation of CTO-based schemes to understand their limitations. Then, we propose two schemes, called the Power Control-based scheme and Femto Relay-based scheme, to overcome this limitation in LTE networks, in which CTO-based schemes are implemented. Via intensive performance evaluation using NS3, we validate the effectiveness of our proposed schemes towards addressing the limitations of CTO-based schemes. Our results demonstrate an improvement in LTE network performance above both the unoptimized and CTO-based schemes with respect to throughput, delay, delay standard deviation (DSD), etc.

Received on 19 December 2018; accepted on 17 June 2019; published on 02 July 2019

Keywords: Wireless communication and networks, LTE networks, Centroid topology optimization, Power control, Femto relay, Performance assessment

doi:10.4108/eai.13-7-2018.159350

1. Introduction

The Long Term Evolution (LTE)-based networks provide broadband wireless communication network infrastructure, which can support high data rate service and numerous smart-world applications (smart home, smart grid, smart manufacturing, and smart health, among others) powered by the Internet of Things (IoT) technology [24, 25, 28, 31, 40, 47–49, 51, 53]. Particularly, the 3rd Generation Partnership Project (3GPP) Long Term Evolution (LTE) and Long-Term Evolution Advanced (LTE-A) have been standardized by mobile network operators (MNOs) for high-speed cellular service [33]. With the adoption of the orthogonal frequency-division multiplexing (OFDM) technique [5, 36], which splits a signal into several narrow band channels with different frequencies, the network operators are able to offer reliable, cost-effective, and low bit rate network services [11].

Nonetheless, with the explosion of connected fixed/mobile devices, the LTE networks are facing a number of challenges with respect to network congestion, radio frequency interference, link health, and others. To address these challenges, centroid topology optimization (CTO)-based schemes [9, 32, 37, 39, 45], which are capable of improving LTE network performance with respect to throughput, delay, delay standard deviation (DSD), packet loss ratio (PLR), signal-to-noise-plus-interference ratio (SNIR), modulation and coding scheme (MCS) index, and corresponding transport block size (TBS), have been widely used. To be specific, a CTO-based scheme is a position computation scheme, which deploys an eNodeB to the center-of-gravity of UEs within their transmission range. In recent years, CTO-based schemes have matured, and have been integrated in practical network topology deployment tools, enhancing network performance before deployment.

Although overall performance improvements of LTE networks can be achieved, one limitation of CTO-based schemes has been largely ignored. When eNodeB and connected UEs are located far away from each other, the

*Corresponding author. Email: Wyu@towson.edu

network topology generated by a CTO-based scheme could incur the risk of link disconnection between them, especially for those UEs located at the edge of eNobeB coverage prior to the CTO-based schemes being implemented. To address this issue, in this study we first evaluate the performance of CTO-based schemes in LTE networks, with respect to throughput, delay, DSD, PLR, SINR, MCS index, and TBS to understand their limitations. We then propose two schemes, called the Power Control-based scheme and Femto Relay-based scheme, to overcome such limitations.

To be specific, in the Power Control-based scheme, we properly control the eNodeB transmission power based on its movement distance to resume UE connections. Note that power control has been considered a viable mechanism to regulate eNodeB transmission coverage so that network performance can be improved. The new power value of the eNodeB is computed by using *Friis Transmission Formula* [2, 20], which describes the relationship between radio transmission power and the distance from transmitter to receiver (eNodeB to UE in LTE networks). Theoretically speaking, the power attenuation is proportional to the square of the distance between transmitter and receiver. In our scheme, we first compute the distance traveled by the eNodeB via applying the CTO-based scheme, from the original position to the relocated position. Then, according to the correlation of the signal power and transmission distance described in *Friis Transmission Formula*, the increased power value can be obtained and is applied to the eNodeB. In this way, the disconnected UEs can be restored.

In the Femto Relay-based scheme, we consider a femto eNodeB within the coverage of a macro eNodeB to relay communication between macro eNodeB and the disconnected UEs. As CTO-based schemes have been proven to be effective in improving the performance of LTE networks, we also adopt CTO to locate the femto eNodeB so that it attains high performance within its own coverage. Particularly, using the CTO-based scheme to locate the femto eNodeB ensures that it is within the coverage of the macro eNodeB. It is clear that the coverage area of eNodeBs can be modeled as a circle over geographical area, and lines (standing for the wireless transmission path) can be drawn between the relocated eNodeB and the disconnected UEs. To determine the femto eNodeB position, we obtain the cross points, in which the coverage circle of the relocated macro eNodeB, and the lines drawn from the UEs that lost coverage to the macro eNodeB, intersect (see Fig. 2 for clarification). The femto eNodeB is then deployed to the center-of-gravity of those cross points. The cross points fall on the edge of the coverage circle, resulting in their centroid being inside the coverage circle. Thus, the femto eNodeB is fully covered by macro eNodeB and the connection of the disconnected UEs can be assured.

To understand the limitations of CTO-based schemes and assess the effectiveness of our proposed Power Control-based and Femto Relay-based schemes, we designed four simulation scenarios, denoted as Original, CTO-based, Power Control, and Femto Relay scenarios, to compare their corresponding network performance in NS3 network simulation tool [4]. The Original simulation scenario deploys LTE networks randomly with the little consideration of UE connectivity, while the CTO-based simulation scenario uses CTO-based schemes to move a macro eNodeB to the center-of-gravity of all UEs. The Power Control-based simulation scenario implements power control based on the CTO-based simulation scenario to resume disconnected UE connections. Finally, the Femto Relay-based simulation scenario places a Femto eNodeB in the coverage of the macro eNodeB, also based on the CTO-based simulation, to relay the communication between eNodeB and disconnected UEs. In addition, the UE distributions in the four scenarios are the same, and are particularly designed to consider the condition, in which several UEs are on the edge of eNodeB transmission coverage. The experimental results demonstrate the limitation of CTO-based schemes regarding UEs at the edge of macro eNodeB coverage, and validates the effectiveness of our proposed Power Control-based and Femto Relay-based schemes in mitigating this limitation with respect to throughput, delay, DSD, PLR, SINR, MCS index, and TBS in LTE networks.

The remainder of this paper is organized as follows: In Section 2, we conduct a literature review of existing relevant research. In Section 3, we introduce the design of our proposed schemes and brief analysis of our schemes and CTO-based scheme. In Section 4, we describe our experimental design. In Section 5, we present our experimentation results to demonstrate the limitations of CTO-based schemes and validate the effectiveness of our proposed schemes. In Section 6, we discuss several remaining issues related to our work. Finally, we conclude the paper in Section 7.

2. Related Works

To improve network performance wireless network such as LTE networks that provide broadband wireless communication for high speed data transmission, connecting heterogeneous local-area networks, and supporting numerous IoT-based smart-world applications (smart grid, smart home, smart manufacturing, smart cities), mission critical service (e.g., public safety) and others [24, 25, 30, 31, 40, 47, 48, 50, 53, 55], a number of research efforts have been conducted [6–8, 10, 12–19, 21–23, 26, 29, 31, 34, 35, 37–39, 41–46, 51, 56–58]. These efforts can be generally divided into categories,

including topology optimization, power management, and relay deployment, among and others (cross-layer design, economic-driven approach, experimental-driven performance assessment, security, etc.).

Topology optimization has been generally adopted in LTE networks to improve network performance with respect to throughput, delay, channel interference, energy economy, and others [9, 32, 35, 37–39, 45]. Generally speaking, topology optimization aims to construct a network topology and further tune related parameters, such as transmission power and radio frequency, to obtain an expected performance gain. Centroid topology optimization (CTO) has been shown to be effective in improving network performance in LTE networks. For example, Nguyen *et al.* [32] presented a center-of-gravity mechanism to optimally position relay nodes for mobile wireless networks. Via the designed scheme, an optimal subset of relay nodes could be derived to maintain a minimum overall distance from relay nodes to mobile nodes. By doing this, the network capacity, delay, and energy consumption can be optimized. Likewise, Chen *et al.* [9] proposed a center-of-gravity-based location selection policy to reduce update cost for a tracking tree construction in wireless networks. In their scheme, the designed policy could efficiently enhance the overall performance of wireless sensor networks.

Power management controls the transmission power of communication endpoints in LTE networks. Here, the goal is to overcome problems related to transmission coverage, network capacity, link health, and others in LTE networks [8, 12, 21, 22, 26, 34, 52, 54]. For example, Li *et al.* [22] proposed a joint power and resource block (RB) allocation (JPRBA) algorithm to alleviate the intra-and-inter-cell interference in LTE-A networks with multi-cell Device-to-Device (D2D) communications. JPRBA allocates an optimal power to D2D transmitter on each RB to solve the average square error minimization problem, such that the throughput of LTE-A networks can be improved. Chaves *et al.* [8] introduced an extra penalization factor (intercell interference related) to LTE uplink (UL) power control, the factor was then used to appropriately reduce the power of LTE UL transmitter. With the mitigation of the inferences between LTE network and Wi-Fi network, the coexistence of LTE and Wi-Fi could be improved. In addition, Yu *et al.* [54] addressed the issue of minimizing the energy cost of base stations in ultr-dense LTE networks through a strategy that can dynamically changing the power saving mode of base stations.

Another viable technique, called relay deployment, achieves a higher network capacity, spectral efficiency and enlarged transmission coverage for LTE networks [16, 23, 27, 29, 38, 45], and the combination of femto eNodeBs and macro eNodeBs is capable of significantly offloading congested traffic and extending communication coverage. For example, Haider *et al.* [16] investigated multiple spectrum partition schemes in LTE networks with mobile femto cells and the experimental data demonstrated that LTE networks with mobile femto cells could achieve higher performance with respect to spectral and energy efficiency. Liu *et al.* [27] employed a transformation strategy, with the consideration of the commercial building features, in which femto eNodeBs are located, to deal with femto eNodeB deployment problems. The developed strategy achieved an optimal femto placement and net shadowing effect deviation.

Unlike the existing schemes outlined, our proposed schemes aims not only to improve the overall network performance of LTE networks, but also to resume connection between macro eNodeBs and isolated UEs disconnected by applying CTO-based schemes. Note that we focus on a single cell with one macro eNodeB in an LTE network in this paper to demonstrate the effectiveness of our schemes. Nonetheless, our proposed schemes can be extended to multiple cells with several eNodeBs. In multiple cell LTE networks, our proposed schemes might consider mutual influence between all the individual cells.

3. Our Schemes

The Power Control-based scheme and Femto Relay-based scheme we proposed aim to solve the limitation of CTO-based scheme.

The CTO-based scheme improves the overall network performance by re-positioning the macro eNodeB to the center-of-gravity of all UEs. New position of eNodeB is computed through the CTO-based scheme. Denote original eNodeB position as (X_o, Y_o), relocated position in the CTO-base scheme as (X_r, Y_r), the position of UEs as (x_i, y_i), $1 < i < N$. The new eNodeB position can be derived by $X_r = \sum_{i=1}^{n} x_i/N$ and $Y_r = \sum_{i=1}^{n} y_i/N$. The moving distance of eNodeB is $\Delta D = \sqrt{(X_r - X_o)^2 + (Y_r - Y_o)^2}$, which is the reason for possible connection broken between eNodeB and partial UEs.

The Power Control-based scheme increases the power of transmitter to resume the communication between eNodeB and the lost UEs in the CTO-base scheme. The movement of eNodeB in the CTO-based scheme might extend the distance between eNodeB and partial far away UEs. Thus, the signal power might be too weak to maintain connections between them. If the received signal power was restored to the former level in initial scheme, the communication would be recovered. The enhanced power is decided by radio path loss and the moving distance of eNodeB. *Friis Transmission Formula* delineates the relationship between radio transmission

power and distance in free space as $P_r = \frac{P_t G_t G_r \lambda^2}{(4\pi d)^2 L}$ [2, 20]. Here, P_t is transmission power (the unit is watt), P_r is reception power (watt), G_t is transmission gain (unitless), G_r is reception gain, λ is wavelength (meter), d is distance (meter), and L is system loss. The reception power P_r has positive correlation with transmission power and negative correlation with distance between transmitter and receiver. The principle of setting new power of eNodeB in Power Control-based scheme is that new transmitter power should recover the furthest receiver's power. We set the increased power as ΔP, the received power of UE on the edge before using the CTO-based scheme as P_{rb}, the transmission range of original macro eNodeB as R. According to the *Friis Transmission Formula*, i.e., $P_{rb} = \frac{P_t G_t G_r \lambda^2}{(4\pi R)^2 L}$. The recovered power of furthest receiver P_{rp} in Power Control-based scheme at least equals to P_{rb}. In this situation, we have $P_{rp} = \frac{(P_t+\Delta P) G_t G_r \lambda^2}{(4\pi D_{max})^2 L}$, where ($D_{max}$ is the distance between furthest disconnection UE with eNodeB in CTO-based scheme). Then, according to $\frac{P_t G_t G_r \lambda^2}{(4\pi R)^2 L} = \frac{(P_t+\Delta P) G_t G_r \lambda^2}{(4\pi D_{max})^2 L}$, the increasing power for eNodeB in Power Control-based scheme is $\Delta P = (\frac{D_{max}^2}{R^2} - 1) P_t$.

The Femto Relay-based scheme solves the disconnection limitation of the CTO-based scheme using a femto eNodeB as relay node. The Femto-eNodeB relay is an efficient technique on the situation that lost UEs scattered within femto eNodeB's connection range. As a relay node, the femto eNodeB needs to be deployed not only connecting to UEs, but also within the macro eNodeB's coverage. We see the macro eNodeB coverage circle and the paths from eNodeB to lost UEs form cross points. The centroid of these points mathematically situates inside the eNodeB transmission range. Thus, femto eNodeB posed on this center-of-gravity guarantees the connection linking macro eNodeB with femto eNodeB. We set femto eNodeB position as (X_f, Y_f), and the position of cross points as (x_k, y_k), $1 < k < M$, where M is the number of lost UEs. The equation for computing the position of femto eNodeB is $X_f = (\sum_{i=1}^{n} x_k)/M$ and $Y_r = (\sum_{i=1}^{n} y_k)/M$.

4. Experimental Design

In the following, we first give an overview of our experimental design. We then explicitly illustrate our experiment setup with respect to *Scope of Experiment*, *Network Simulation Scenarios*, and *Original System Parameters*, respectively.

4.1. Overview

In our experiments, we adopt the discrete-event network simulator NS3 to set up our LTE simulation environment. It is an open source and widely used simulation platform in networking research and education [4]. Particularly, NS3 consists of sophisticated LTE network modules and corresponding modules for network performance data collection. In addition, it provides a tracing and statistical component to customize the output data regarding LTE network performance. Note that NS3 allows designers to create and configure network nodes, network channels, network devices, and network applications separately, which makes the network protocol levels and structures more clear.

In general, we build a single macro cell LTE network in NS3 as the basic network infrastructure. The single cell consists of one macro eNodeB and thirty UEs, which are within the macro eNodeB coverage. All the UEs are properly placed in three different ways: (i) two UE groups (five UEs in each) are deployed in buildings, (ii) three UEs at the coverage edge, and (iii) seventeen UEs dispersed uniformly in the coverage area. In this experiment, we aim to evaluate the limitations of centroid topology optimization (CTO)-based schemes and further validate the effectiveness of our proposed Power Control-based and Femto Relay-based schemes to mitigate such limitations.

To this end, we first construct one LTE network without a CTO-based scheme and one with a CTO-based scheme to investigate the limitation of CTO-based schemes, regarding throughput, delay, DSD, PLR, SINR, MCS index, and TBS. We then integrate the Power Control-based and Femto Relay-based schemes into the LTE network, in which CTO-based schemes have been implemented. By doing this, we can evaluate the performance improvement of our proposed schemes and their capability in mitigating the limitations of CTO-based schemes. Further, we consider scenarios, including the LTE network without CTO, LTE network with CTO, LTE network with Power Control and CTO, and LTE network with Femto Relay and CTO.

4.2. Scope of Experiment

In our experiment, the following key metrics are used to evaluate the performance of LTE networks, defined below:

- **Throughput.** It is defined as the number of bytes that a UE receives from macro eNobeB per second. The macro eNobeB keeps sending out data packets at a configurable rate, while the UEs receive the packets irregularly according to the physical link quality. This feature properly demonstrates the received packets of one UE in a unit time on the packet data convergence protocol (PDCP) layer.

- **Delay.** It is measured as the average transmitting time of packets from macro eNobeB to UEs. The delay metric is collected from PDCP layer, which

means that delay is counted from the moment when one packet is handed over from macro eNodeB PDCP layer to radio link control (RLC) layer until the moment when the UE PDCP layer receives the packet.

- **Delay Standard Deviation.** The standard deviation of delay indicates the stability of packet transmitting time in LTE networks. This metric is based on experimental data from PDCP layer.
- **Packet Loss Ratio.** It is the ratio between actual received data bytes at the UEs and the total transmitted data bytes from the macro eNodeB, per second. This metric is based on experimental data from PDCP layer as well.
- **SINR.** This stands for Signal-to-Interference-plus-Noise Ratio and is commonly used in wireless networks to measure link quality. In our experiment, SINR shows the average communication link quality between macro eNobeB and UE, and it is gathered from the physical (PHY) layer.
- **MCS Index.** It indicates the modulation type and coding rate, which are used in a given physical resource block (PRB) and reflect the quality of current radio conditions. Generally speaking, the higher the MCS index value is, the more bits can be transmitted per unit time. To be specific, a UE measures the radio channel quality and sends a channel quality indicator (CQI) to macro eNobeB, and then macro eNobeB selects MCS index value based on the current radio conditions. MCS index is collected from the media access control (MAC) layer.
- **Transport Block Size (TBS).** It shows how many bits in the transport blocks are sent from macro eNodeB onto the physical link in one millisecond. The transport block size (TBS) is determined by MCS index value and the number of resource blocks assigned to UE. The larger the TBS value is, the higher the transmission traffic will be. TBS value is collected from the MAC layer.

4.3. Network Simulation Scenarios

In order to understand the limitations of CTO-based schemes in LTE networks, we set up an Original scenario, upon which CTO-based schemes and the proposed remedy schemes are enacted. In the Centroid scenario, the CTO-based scheme is applied to the original scheme configuration, but without our schemes in place. Next, we create two additional scenarios, denoted as Power and Femto scenarios, to validate the effectiveness of our proposed schemes, called Power Control-based and Femto Relay-based schemes, on overcoming the limitations of CTO-based schemes. We now introduce all of the network simulation scenarios in detail.

Original Scenario. As shown in Fig. 1, the Original scenario implements an LTE network without the application of a CTO-based scheme or any of the proposed remedy schemes. In this scenario, the LTE network is constructed of one macro eNodeB and thirty UEs. The macro eNodeB is placed stochastically and there are two hot spots, each of which covers five UEs randomly dispersed inside buildings. Three UEs are positioned (according to predefined coordinates) on the edge of the macro eNodeB's transmission range, the remaining UEs are randomly distributed within the coverage of the macro eNodeB. Each of the UEs maintains a transmission link with the macro eNodeB, which sends data packets to UEs at a constant rate.

Centroid Scenario. In this scenario, as shown in Fig. 2, we extend the Original scenario by redeploying the macro eNodeB to the center-of-gravity of all UEs by using the CTO-based scheme, while all the positions of UEs remain the same as in the Original scenario. We demonstrate this scenario to compare the LTE network performance with that of the Original scenario, regarding the seven key metrics defined in Section 4.2, and therefore to specifically evaluate the communication deterioration of those UEs on the edge of the macro eNodeB's transmission coverage as a result of CTO-based schemes. The disconnection between macro eNodeB and UEs might occur due to the relocation of macro eNodeB using the CTO-based schemes, in which the coordinates of the macro eNodeB are set up as the average of all UEs' x coordinates and the average of all UEs' y coordinates separately by using the CTO-based scheme. Please refer to Algorithm 1 for the detail procedure of CTO-based schemes.

Algorithm 1 : Centroid Topology Optimization

Require: Number of UEs N and UE positions (x_i, y_i)
Ensure: eNodeB position (X_r, Y_r)
  $x \Leftarrow 0$
  $y \Leftarrow 0$
  while $1 \leq i \leq N$ **do**
    $x \Leftarrow x + x_i$
    $y \Leftarrow y + y_i$
  end while
  $X_r \Leftarrow x/N$
  $Y_r \Leftarrow y/N$

Power Scenario. As shown in Fig. 3, the Power scenario applies our proposed power control scheme to the LTE network constructed in the Centroid scenario, such that the disconnection issue of CTO-based schemes can be addressed. The primary purpose of this scenario is to add an appropriate amount of transmission power to the macro eNodeB, such that

the communication links between the macro eNodeB and the disconnected UEs can be restored. In addition, the amount of incremental transmission power for macro eNodeB should be properly limited, so as to avoid the coverage overlap with other macro cells and waste power resources. In our proposed Power Control-based scheme, the power increment is computed by applying *Friis Transmission Formula* to the moving distance of the macro eNodeB from the Original to the Centroid scenario. According to *Friis Transmission Formula* [2, 20], the received transmission power of a UE is inversely proportional to the square of the distance between macro eNodeB and UE. Thus, we select the required power increment for macro eNodeB to resume the communication between macro eNodeB and the furthest disconnected UE as the actual power increment. Algorithm 2 illustrates the detailed procedure of the power increment determination for the macro eNodeB in our Power Control-based scheme.

Algorithm 2 : Power Enhancement

Require: Original eNodeB transmission power P_t, Number of disconnected UEs N_d and their positions (x_j^d, y_j^d), Position of the relocated eNodeB (X_r, Y_r), and Original eNodeB transmission range R
Ensure: eNodeB transmission power increment ΔP
Expression for distance between relocated eNodeB and the j^{th} disconnected UE: $D_j = \sqrt{(x_j^d - X_r)^2 + (y_j^d - Y_r)^2}$
while $1 \leq j \leq N_d$ **do**
$D_{max} \Leftarrow max(D_j)$
end while
$\Delta P \Leftarrow (\frac{D_{max}^2}{R^2} - 1)P_t$
Get new eNodeB transmission power: $P_n \Leftarrow \Delta P + P_t$
Set eNodeB power attribute as a command line parameter P_n
In script program:
Set $P_n = \Delta P + P_t$: ./waf –run "ns3-program –P_n"

Femto Scenario. In this scenario, as shown in Fig. 4, we deploy a femto eNodeB (working as a relay node between macro eNodeB and disconnected UEs) by using our proposed Femto Relay-based scheme in the LTE network built in the Centroid scenario. In the Femto Relay-based scheme, the position of femto eNodeB needs to meet the following two criteria so that the disconnected UEs of the CTO scheme can be mitigated. First, the femto eNodeB must be within the transmission range of the macro eNodeB. Second, the femto eNodeB coverage must also encompass the disconnected UEs to ensure connection recovery.

With the consideration of those two requirements, we first obtain the cross points of the macro eNodeB's coverage circle with the lines connecting the macro eNodeB and disconnected UEs. We then apply an additional CTO-based scheme to the coordinates of those cross points to identify the position for femto eNodeB. Note that the cross points are located on the edge of the transmission coverage circle of the macro eNodeB. This ensures that the center-of-gravity of the cross points can fall inside the coverage of the macro eNodeB's transmission range. At the same time, the cross points have relatively short distances from the disconnected UEs, and the center-of-gravity of those cross points likewise has relatively short distances to the disconnected UEs. Thus, the shorter distance between the femto eNodeB and the disconnected UEs ensures that the disconnected UEs from the CTO-based scheme would be reconnected. The detailed procedure of how to deploy femto eNodeB is illustrated in Algorithm 3.

Algorithm 3 : Femto Relay

Require: Number of disconnected UEs N_d and their positions (x_k^d, y_k^d), eNodeB transmission range R
Ensure: Femto eNodeB position (X_f, Y_f)
Equation for the circle centered in (X, Y):
$(x - X)^2 + (y - Y)^2 = R^2$
Equation for the line across (X, Y) and k^{th} disconnected UE:
$(y - Y) = \frac{Y - y_k^d}{X - x_k^d}(x - X)$
Assume (x_k^c, y_k^c) the cross point of k^{th} line and the circle
$x_{avg} \Leftarrow 0$
$y_{avg} \Leftarrow 0$
while $1 \leq k \leq N_d$ **do**
$x_{avg} \Leftarrow x_{avg} + x_k^c$
$y_{avg} \Leftarrow y_{avg} + y_k^c$
end while
$X_f \Leftarrow x_{avg}/N_d$
$Y_f \Leftarrow y_{avg}/N_d$

4.4. System Setting

To simulate the degraded state of the communication links between macro eNodeB and all UEs, especially those located on the edge of macro eNodeB's transmission range, after applying the CTO-based schemes in the LTE network, we introduce an unbalanced distribution of UEs. In our unbalanced LTE network setup, two hot spots consist of groups of UEs (five UEs per group) are placed into two separate three floor buildings. There are also seventeen UEs randomly dispersed within the coverage of the macro eNobeB. Particularly, three UEs are deployed on the edge of the macro eNodeB's transmission coverage area, and the UE positions are generated according to predefined coordinates with the consideration of macro eNobeB transmission power. With this unbalanced property, the center-of-gravity to which the macro eNodeB relocates in the CTO-based scheme will have a high probability of moving away from edge UEs. Thus, some UEs will likely be located outside of the macro eNodeB's transmission coverage, and the disconnection issue of CTO-based schemes will occur.

In our LTE network simulation, macro eNobeB transmits data at a constant rate in the application

layer, and the data is encapsulated into each packet using UDP protocol in the transport layer and further delivered to the LTE network layers to send out. In addition, the transmission power of a macro eNobeB is configured to 42 dBm, and the transmission power of UEs is set to 23 dBm. These two power values are selected from the typical values normally used to set transmission powers for macro eNodeB and UE in LTE networks [3]. The macro eNodeB transmits data with 100 ms as the inter packet interval, 1024 kbps as the data rate, and 512 bytes as the transmission packet size. Moreover, parameters such as Earfcn (Evolved-UTRA Absolute Radio Frequency No.), channel bandwidth, transmission bandwidth, etc., are all set to the default values in NS3 [1].

In addition, the transmission power of macro eNodeB in our proposed power enhancement scheme is increased according to Algorithm 2 in Section 4.3, in this case reaching 46 dBm based on the CTO scheme. In the Femto Relay-based scheme, macro eNodeB and femto eNodeB communicate via *X2 Interface*. During the simulation, macro eNodeB is attached to Backhaul network through P2P protocol, and LTE transmission mode is set as Single Input Single Output (SISO).

5. Performance Evaluation

In this section, we provide and analyze our LTE network evaluation results regarding the seven key metrics (throughput, delay, DSD, PLR, SINR, MCS index, and TBS) defined in Section 4.2. The experimental results are collected from the designed network simulation scenarios (original, centroid, power, and Femto scenarios) illustrated in Section 4.3, and all the scenarios are implemented on a single macro cell LTE network using NS3.

Our evaluation aims to investigate the limitations of CTO-based schemes and the effectiveness of our proposed schemes. In terms of the limitations of CTO-based schemes, the disconnection issue of CTO-based schemes can be identified by comparing the network performance of the original and centroid network simulation scenarios in Figures 5 to 11. In the evaluation of our proposed schemes (Power Control-based and Femto Relay-based), their effectiveness in overcoming the disconnection issue raised by CTO-based schemes, and in improving the overall network performance, can be observed by comparing the network performance with the original and centroid network scenarios in Figures 12 to 18. We now review the results indicated in each of the figures individually.

5.1. Limitation of CTO-Based Schemes

Fig. 5 illustrates the average throughput of each UE in original and centroid network simulation scenarios. Although the network throughput of most UEs in Centroid scenario is much higher than that of UEs in Original scenario, there are three UEs on the edge of macro eNodeB transmission coverage, losing connection to macro eNodeB, indicated by their throughput decreasing to zero. This implies that the CTO-based schemes could lead to the disconnection of UEs at some positions (edge of the coverage) although the CTO-based schemes can improve overall network throughput in LTE networks.

Fig. 6 shows the average delay for both network simulation scenarios, and it is the average transmission time between macro eNobeB and UE. In this figure, we use four seconds to represent infinite delay. As we can see from the figure, the CTO-based schemes can effectively reduce the average packet transmission delay for most UEs in regular positions. Nonetheless, the three UEs with a fragile connection state, upon the macro eNodeB changing positions, eventually lose connection due to the relocation by the CTO-based scheme. Thus, we further confirm the disconnection issue that can be raised by the CTO-based schemes.

Fig. 7 evaluates the stability of transmission delay between macro eNodeB and UEs. As shown in the figure, the delay standard deviations for most UEs in the Centroid scenario are less than those in the Original scenario. In combination with Fig. 6, we can see that the CTO-based schemes not only reduce transmission delay, but also improve the stability of LTE networks, in general. Nonetheless, the three UEs on the edge of macro eNodeB's transmission range achieve the delay standard deviations of zero. This is because the transmission delay of all three UEs is infinity, and no change appears. This figure also confirms the disconnection issue raised by CTO-based schemes.

Fig. 8 illustrates the ratio of lost packets (from macro eNodeB to UE) to the total transmitted packets, which the macro eNodeB sends out. In the figure, the packet loss ratio of all UEs in the Original scenario is above 0.7, while the packet loss ratio of UEs is below 0.5 in the Centroid scenario, again excepting the three edge UEs whose packet loss ratio reaches 1. This one hundred percent packet loss ratio implies that all the packets transmitted from macro eNobeB are not received by the three particular destination UEs. Again, confirming the disconnection issue raised by the CTO-based schemes.

Fig. 9 shows that the SINR of most links between macro eNodeB and UEs in the Centroid scenario is higher than that of the links in Original scenario, implying that the link health is better in the Centroid scenario but for the three specially located UEs. As we can see from the figure, the SINR values of the three edge UEs all decrease to zero, which indicates the disconnection between them and the macro eNodeB. The disconnection issue of CTO schemes is therefore confirmed.

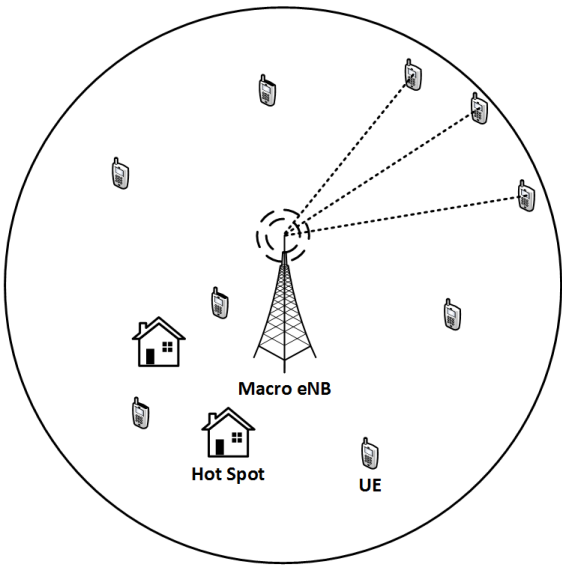

Figure 1. Original Scenario

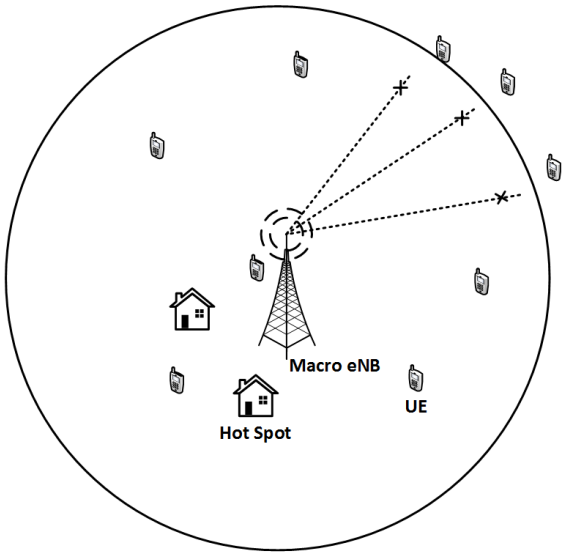

Figure 2. Centroid Scenario

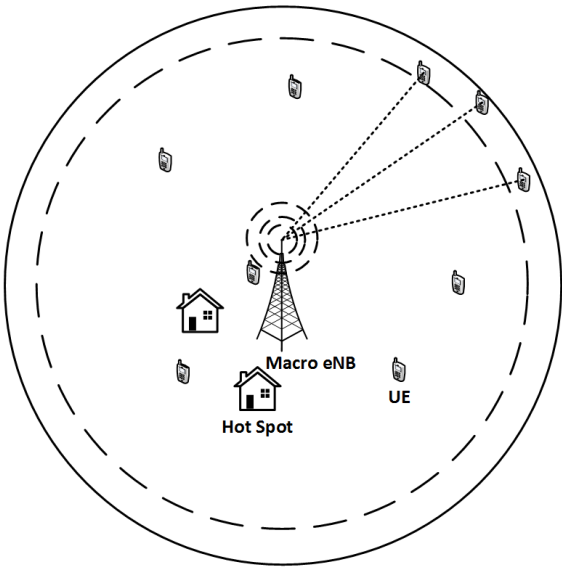

Figure 3. Power Enhancement Scenario

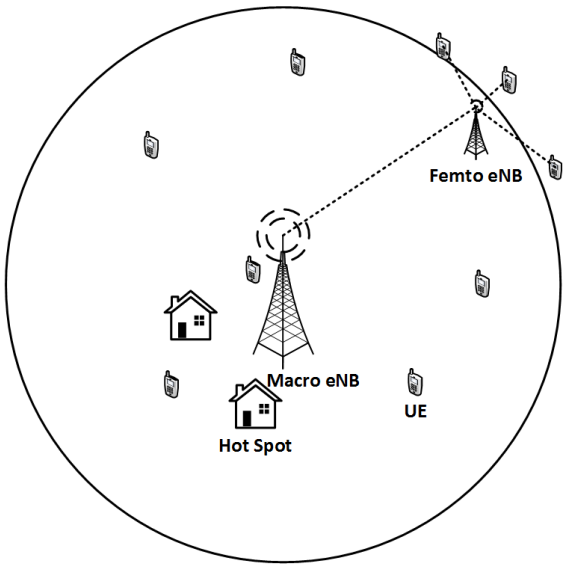

Figure 4. Femto Relay Scenario

Fig. 10 and Fig. 11 compare MCS indices and TBS in the original and Centroid scenarios. Except for the three edge UEs, in general, the UEs attain better network performance with higher MCS indices and TBS values in the Centroid scenario. The MSC index and TBS values of the three edge UEs, however, approximately equal zero.

With the analysis of the simulation results, regarding throughput, delay, DSD, PLR, SINR, MCS index, and TBS, we identify the expected disconnection issue raised by CTO-based schemes in LTE networks. Although the improvement of network performance can be achieved, CTO-based schemes still have issues to be resolved.

5.2. Effectiveness of Proposed Schemes

Based on the investigated limitation of CTO-based schemes in Section 5.1, we confirm that the CTO-based schemes may result in the disconnection between

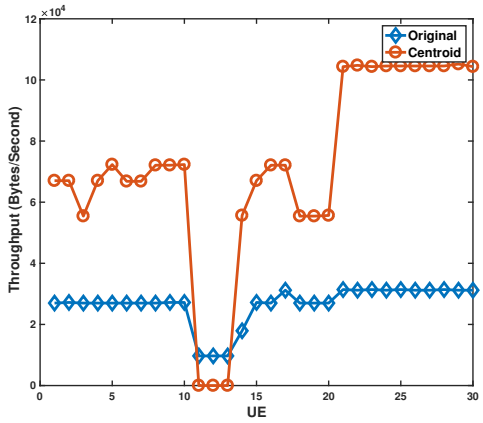

Figure 5. Throughput Performance vs. Number of UEs

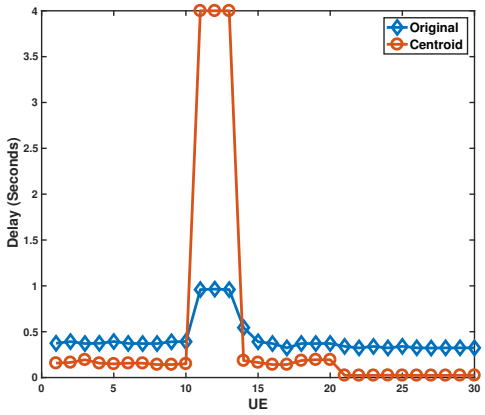

Figure 6. Delay Performance vs. Number of UEs

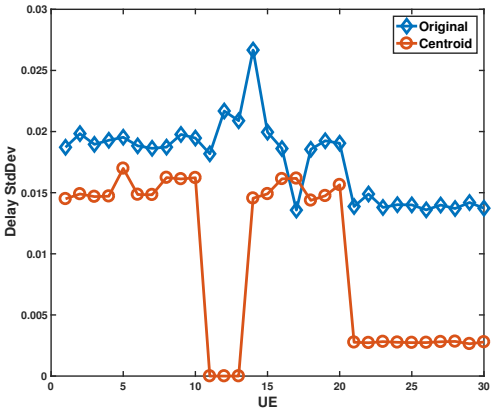

Figure 7. Standard Deviation of Delay Performance vs. Number of UEs

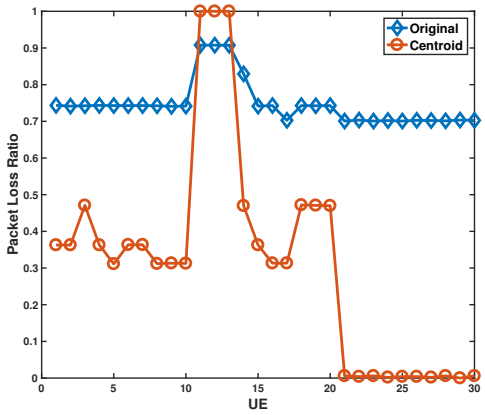

Figure 8. Packet Loss Ratio vs. Number of UEs

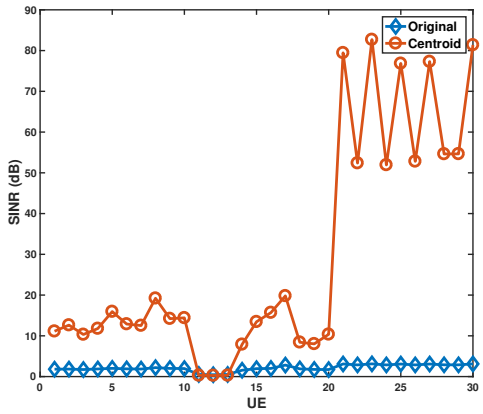

Figure 9. SINR Performance vs. Number of UEs

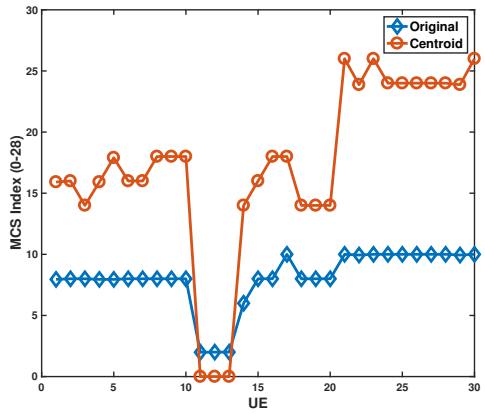

Figure 10. MCS Index vs. Number UEs

macro eNodeB and UEs on the edge of macro eNodeB transmission coverage. We simulate the Power scenario and Femto scenario to evaluate the performance of our proposed schemes, namely, Power Control-based and Femto Relay-based. The simulation results in Figures 12 to 18 exhibit the network performance regarding throughput, delay, DSD, PLR, SINR, MCS index, and TBS for all network simulation scenarios (Original, Centroid, Power, and Femto scenarios). Our experimental results demonstrate that both Power Control-based and Femto Relay-based schemes can

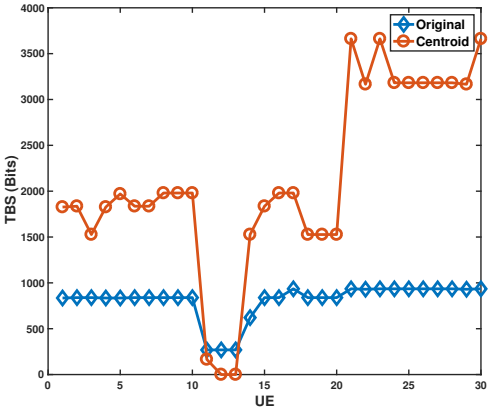

Figure 11. TBS vs. Number UEs

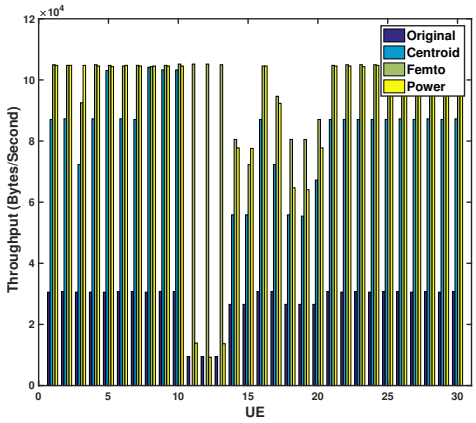

Figure 12. Throughput vs. Number UEs

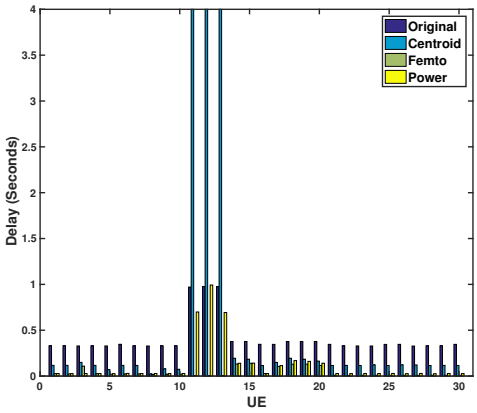

Figure 13. Delay vs. Number UEs

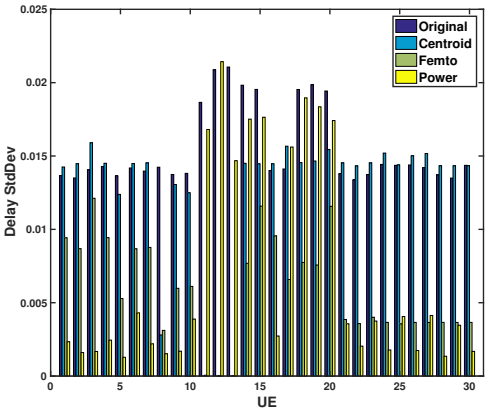

Figure 14. Standard Deviation of Delay vs. Number UEs

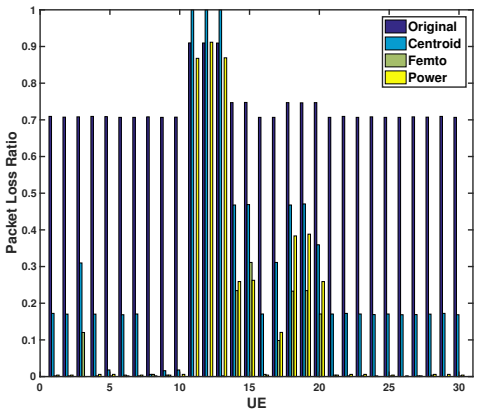

Figure 15. Packet Loss Ratio vs. Number UEs

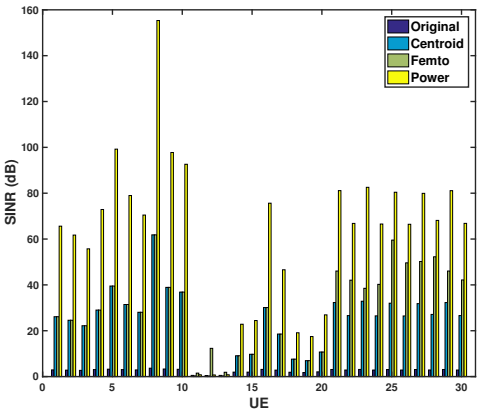

Figure 16. SINR vs. Number UEs

effectively resolve the disconnection issue of CTO-based schemes and further improve the overall network performance of LTE networks.

Fig. 12 illustrates that both Power Control-based and Femto Relay-based schemes can properly recover the disconnected communication between the macro eNodeB and the three edge UEs, and that the overall LTE network throughput is highly improved at the same time. To be specific, the network throughput of the three edge UEs in the Power scenario reaches at or above the network throughput performance of the baseline Original scenario. Even more promising

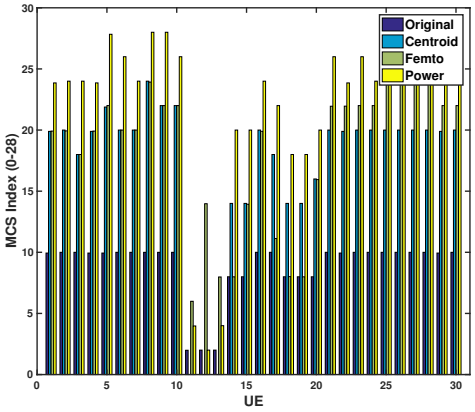

Figure 17. MCS Index vs. Number UEs

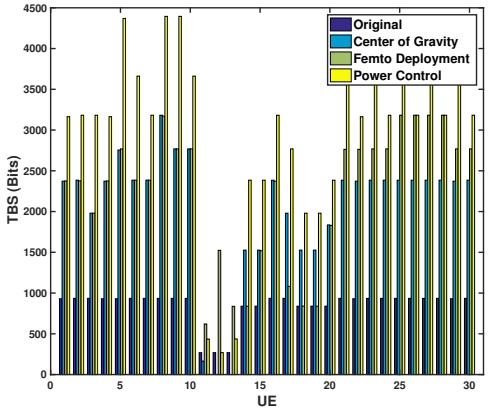

Figure 18. TBS vs. Number UEs

though, the network throughput of the three UEs in the Femto scenario is significantly higher than that of UEs in baseline Original scenario, even exceeding the performance of most UEs in the Centroid scenario.

In Fig. 13, we again use four seconds to represent infinite packet transmission delay in the Centroid scenario. As we can see from the figure, the transmission delay in the Power scenario is similar to the one in the Original scenario, and the transmission delay really nears zero in the Femto scenario. This implies that both Power Control-based and Femto Relay-based schemes can reduce transmission delay for the three disconnected UEs from infinity in the Centroid scenario to a level that is below the transmission delay in the Original scenario. Thus, the disconnection problem of CTO-based schemes is addressed by our proposed Power Control-based and Femto Relay-based schemes.

Fig. 14 demonstrates the stability of transmission delay from macro eNobeB to UE. In this figure, the delay standard deviations between eNodeB and the three disconnected UEs are zero in Centroid scenario, because delay remains infinity for the disconnected links. Nonetheless, in the Power scenario, the delay standard deviations between eNodeB and the edge UEs are raised up to and even above the performance level of the Original scenario. Note that the delay standard deviations of the three edge UEs in the Femto scenario are all approximately equal to zero, this is because the packet transmission between the femto eNodeB and the three edge UEs has nearly no delay.

In Fig. 15, the packet loss ratio decreases from 1 in the Centroid scenario to about 0.85-0.90 in the Power scenario, approximately equaling those three UEs in the Original scenario. In addition, the packet loss in the Power scenario is much smaller then the Original scenario for all other UEs. This indicates that the Power Control-based scheme can restore the connection between macro eNodeB and disconnected UEs in the Centroid scenario. In the Femto scenario, the packet loss ratio approaches zero, indicating the recovery of and improvement on the communication between macro eNodeB and disconnected UEs in Centroid scenario.

Fig. 16 indicates that the SINR values of the communication link between macro eNodeB and the three edge UEs are less than 5 dB in the Original scenario, which implies the poor quality of physical links. Nonetheless, in the Power scenario, the SINR values are increased from zero in the Centroid scenario back to and even above those in the Original scenario. Similarly, in the Femto scenario, the SINR values are well above those of the Original scenario.

Comparing Fig. 17 to Fig. 18, we compare MCS indices and TBS values for all network simulation scenarios. To be specific, the MCS index values for the three edge UEs in the Original scenario are consistent at 2, while the TBS values for the same UEs are around 200 bits. In the Centroid scenario, both metrics decrease to zero for the three edge UEs because of the disconnection between them and macro eNodeB. Nonetheless, after applying the Power Control-based and the Femto Relay-based schemes, the MCS indices and TBS values both reach above those in the Original scenario. This implies that the LTE link quality between macro eNodeB and the UEs in challenging positions is not only resumed, but also improved upon by our proposed two schemes.

To summarize, Figures 12 to 18 compare the network performance of all simulation scenarios, and validate both the Power Control-based and Femto Relay-based schemes in effectively overcoming the disconnection issue of CTO-based schemes in LTE networks. Furthermore, both proposed schemes improve the LTE network performance in comparison with both the Original and Centroid scenarios.

6. Discussion

We now discuss some of the design tradeoffs of our proposed schemes.

As shown above, both schemes can effectively address the disconnection problem of CTO-based schemes, and can significantly improve LTE network performance, though their degrees of efficiency might be different when they are applied to different LTE networks with diverse topologies. Based on the UE distribution, LTE network topology can be classified into two categories: uniform and unbalanced topologies. In uniform LTE network topologies, UEs are dispersed evenly across the whole transmission coverage area and barely pack into a crowded space. In contrast, in unbalanced LTE network topologies, a group of UEs might gather around one single spot, or be vacant from other areas.

In a uniform LTE topology with sparse UEs, the communication between the macro eNodeB and disconnected UEs might not be recovered completely by only one femto eNodeB, due to the power constraints of the femto eNodeB and the diverse distances between macro eNodeB and disconnected UEs. In the worst case, one femto eNodeB might only restore one communication link between macro eNodeB and disconnected UE, which results in the deployment of multiple femto eNodeBs. To achieve cost efficiency and avoid multiple femto eNodeBs deployment, it is more appropriate to adopt Power Control-based scheme, which solves the disconnection problem by only increasing the transmission power of one single macro eNodeB.

In an unbalanced LTE topology with UE clusters, one femto eNodeB might have enough power to restore all the communication links between macro eNodeB and disconnected UEs, which are crowded as clusters in hot spots. Furthermore, the proximity between the femto eNodeB and disconnected UEs can improve network performance in terms of delay and packet loss ratio, which are highly related to distance. Thus, the Femto Relay-based scheme can be considered as a proper choice in this case. The Power Control-based scheme, however, does not shorten the transmission distance between macro eNodeB and disconnected UEs in the same way as the Femto Relay-based scheme does. Thus, the link quality still cannot be assured by limited power control. It is often better to choose the femto relay instead of power control for unbalanced LTE topologies to resume communication.

In addition, our proposed schemes have focused only on single cell LTE networks. Note that power control and femto relay can both be extended to multi-cells with the consideration of mutual influence between macro eNodeBs. The two schemes might also be used at the same time to deal with the disconnection issue of CTO-based schemes in multi-cell LTE networks. As UE topologies in different macro cells vary, Power Control-based and Femto Relay-based schemes might be applied accordingly, as discussed above. In some special cases, one macro eNodeB cell with uniform topology might move directly to the disconnected area of another eNodeB cell with unbalanced topology after applying a CTO-based scheme. Thus, the disconnection area of the cell with unbalanced topology could be properly covered by removing the eNodeB of the cell with uniform topology. Then, we only need to increase the amount of power of the uniform topology eNodeB with to resume its disconnected UEs.

7. Final Remarks

In this paper, we addressed the performance issue of Long Term Evolution (LTE)-based networks, which provide broadband wireless communication network infrastructure for numerous IoT-based smart-world applications and high speed data transmission. Particularly, we first investigated the disconnection issue of CTO-based schemes in LTE networks, and then proposed two schemes, namely the Power Control-based and Femto Relay-based schemes, to overcome such a limitation. With the adoption of CTO-based schemes in LTE networks, UEs on the edge of the eNodeB transmission range can lose connection to the eNodeB due to its relocation. To this end, our proposed *Power Control scheme* increases the transmission power of the macro eNodeB, which increases its transmission coverage and therefore restores connection between eNodeB and disconnected UEs. As to the *Femto Relay-based scheme*, we deployed a femto eNodeB within the macro eNodeB transmission coverage area to resume the connection between the macro eNodeB and the disconnected UEs. The deployment position of the femto eNodeB is identified as the center-of-gravity of the UE/coverage zone cross points, which are the intersections of the macro eNodeB coverage circle and the lines between macro eNodeB and disconnected UEs. Our extensive experimental results validate the effectiveness of our proposed two schemes, with respect to throughput, delay, DSD, PLR, SINR, MCS index, and TBS. In addition, we discussed some of the design tradeoffs of our proposed schemes.

References

[1] Configuration of lte model parameters. https://www.nsnam.org/docs/models/html/lte-user.html. Accessed Dev 15, 2018.

[2] Propagation. https://www.nsnam.org/docs/models/html/propagation.html. Accessed Dev 15, 2018.

[3] Lte; evolved universal terrestrial radio access (e-utra); user equipment (ue) radio transmission and reception. *3GPP Standard*, (TS 36.101 release 14), 2017.

[4] Ns-3: Network simulator. https://www.nsnam.org/, Retrieved December 1, 2018.

[5] E. Basar. On multiple-input multiple-output OFDM with index modulation for next generation wireless networks. *IEEE Transactions on Signal Processing*, 64(15):3868–3878, 2016.

[6] M. P. Bendsøe, O. Sigmund, M. P. Bendsøe, and O. Sigmund. *Topology optimization by distribution of isotropic material*. Springer, 2004.

[7] S. Bhattarai, S. Rook, L. Ge, S. Wei, W. Yu, and X. Fu. On simulation studies of cyber attacks against lte networks. In *2014 23rd International Conference on Computer Communication and Networks (ICCCN)*, pages 1–8, Aug 2014.

[8] F. S. Chaves, E. P. Almeida, R. D. Vieira, A. M. Cavalcante, F. M. Abinader, S. Choudhury, and K. Doppler. LTE UL power control for the improvement of LTE/Wi-Fi coexistence. In *Vehicular Technology Conference (VTC Fall), 2013 IEEE 78th*, pages 1–6. IEEE, 2013.

[9] M.-X. Chen and Y.-D. Wang. An efficient location tracking structure for wireless sensor networks. *Computer Communications*, 32(13):1495–1504, 2009.

[10] S. Chen and J. Zhao. The requirements, challenges, and technologies for 5G of terrestrial mobile telecommunication. *IEEE Communications Magazine*, 52(5):36–43, 2014.

[11] E. Dahlman, S. Parkvall, and J. Skold. *4G, LTE-advanced Pro and the Road to 5G*. Academic Press, 2016.

[12] H. ElSawy, E. Hossain, and M.-S. Alouini. Analytical modeling of mode selection and power control for underlay d2d communication in cellular networks. *IEEE Transactions on Communications*, 62(11):4147–4161, 2014.

[13] R. Ferrus and O. Sallent. Extending the ltelte-a business case: Mission- and business-critical mobile broadband communications. *IEEE Vehicular Technology Magazine*, 9(3):47–55, Sep. 2014.

[14] W. Gao, J. H. Nguyen, W. Yu, C. Lu, D. T. Ku, and W. G. Hatcher. Toward emulation-based performance assessment of constrained application protocol in dynamic networks. *IEEE Internet of Things Journal*, 4(5):1597–1610, Oct 2017.

[15] F. Ghavimi and H.-H. Chen. M2M communications in 3GPP LTE/LTE-A networks: architectures, service requirements, challenges, and applications. *IEEE Communications Surveys & Tutorials*, 17(2):525–549, 2015.

[16] F. Haider, C.-X. Wang, B. Ai, H. Haas, and E. Hepsaydir. Spectral/energy efficiency tradeoff of cellular systems with mobile femtocell deployment. *IEEE Transactions on Vehicular Technology*, 65(5):3389–3400, 2016.

[17] A. Hematian, W. Yu, D. Griffith, and N. Golmie. Performance assessment of smart meter traffic over lte network using sdr testbed. In *Proc. of IEEE International Conference on Computing, Networking and Communications (ICNC)*, 2019.

[18] K. Hua, Y. Zhu, W. Wang, and H. Wang. Cross-layer design for optimal throughput of wireless networks. In *Proceedings of the 2014 Conference on Research in Adaptive and Convergent Systems*, RACS '14, pages 204–208, New York, NY, USA, 2014. ACM.

[19] J. Huang, Y. Yin, Y. Zhao, Q. Duan, W. Wang, and S. Yu. A game-theoretic resource allocation approach for intercell device-to-device communications in cellular networks. *IEEE Transactions on Emerging Topics in Computing*, 4(4):475–486, Oct 2016.

[20] S. G. Kim, J. H. Kim, D. Kim, W. S. Lee, W. Jang, and E. Choi. A novel method for power measurement of a short pulse gyrotron using friis transmission formula at w-band. In *Infrared, Millimeter, and Terahertz waves (IRMMW-THz), 2015 40th International Conference on*, pages 1–1. IEEE, 2015.

[21] N. Lee, X. Lin, J. G. Andrews, and R. W. Heath Jr. Power control for d2d underlaid cellular networks: Modeling, algorithms, and analysis. *IEEE Journal on Selected Areas in Communications*, 33(1):1–13, 2015.

[22] X.-Y. Li, J. Li, W. Liu, Y. Zhang, and H.-S. Shan. Group-sparse-based joint power and resource block allocation design of hybrid device-to-device and LTE-advanced networks. *IEEE Journal on Selected Areas in Communications*, 34(1):41–57, 2016.

[23] Z. Liao, J. Liang, and C. Feng. Mobile relay deployment in multihop relay networks. *Computer Communications*, 112:14–21, 2017.

[24] J. Lin, W. Yu, X. Yang, Q. Yang, X. Fu, and W. Zhao. A novel dynamic en-route decision real-time route guidance scheme in transportation cyber-physical systems. *IEEE Transactions on Vehicular Technology (TVT)*, 66(3):2551–2566, 2017.

[25] J. Lin, W. Yu, N. Zhang, X. Yang, H. Zhang, and W. Zhao. A survey on Internet of Things: Architecture, enabling technologies, security and privacy, and applications. *IEEE Internet of Things Journal*, PP(99), 2017.

[26] S. Lin, F. Miao, J. Zhang, G. Zhou, L. Gu, T. He, J. A. Stankovic, S. Son, and G. J. Pappas. Atpc: adaptive transmission power control for wireless sensor networks. *ACM Transactions on Sensor Networks (TOSN)*, 12(1):6, 2016.

[27] J. Liu, T. Kou, Q. Chen, and H. D. Sherali. Femtocell base station deployment in commercial buildings: A global optimization approach. *IEEE Journal on selected areas in communications*, 30(3):652–663, 2012.

[28] X. Liu, C. Qian, W. G. Hatcher, H. Xu, W. Liao, and W. Yu. Secure internet of things (iot)-based smart-world critical infrastructures: Survey, case study and research opportunities. *IEEE Access*, pages 1–1, 2019.

[29] R. Madan, J. Borran, A. Sampath, N. Bhushan, A. Khandekar, and T. Ji. Cell association and interference coordination in heterogeneous LTE-A cellular networks. *IEEE Journal on Selected Areas in Communications*, 28(9):1479–1489, 2010.

[30] V. Marojevic, R. M. Rao, S. Ha, and J. H. Reed. Performance analysis of a mission-critical portable lte system in targeted rf interference. In *2017 IEEE 86th Vehicular Technology Conference (VTC-Fall)*, pages 1–6, Sep. 2017.

[31] P. Moulema, W. Yu, D. Griffith, and N. Golmie. On effectiveness of smart grid applications using co-simulation. In *2015 24th International Conference on Computer Communication and Networks (ICCCN)*, pages 1–8, Aug 2015.

[32] J. Nguyen, Y. Wu, W. Gao, W. Yu, C. Lu, and D. Ku. On optimal relay nodes position and selection for multi-path data streaming. In *Wireless Communications and Networking Conference (WCNC), 2017 IEEE*, pages 1–6.

IEEE, 2017.

[33] E. Pateromichelakis, M. Shariat, A. ul Quddus, and R. Tafazolli. On the evolution of multi-cell scheduling in 3GPP LTE/LTE-A. *IEEE Communications Surveys & Tutorials*, 15(2):701–717, 2013.

[34] R. Ratasuk, J. Tan, and A. Ghosh. Coverage and capacity analysis for machine type communications in LTE. In *Vehicular Technology Conference (VTC Spring), 2012 IEEE 75th*, pages 1–5. IEEE, 2012.

[35] A. S. Shafigh, B. Lorenzo, S. Glisic, J. Pérez-Romero, L. A. DaSilva, A. B. MacKenzie, and J. Röning. A framework for dynamic network architecture and topology optimization. *IEEE/ACM Transactions on Networking*, 24(2):717–730, 2016.

[36] C. Shahriar, M. La Pan, M. Lichtman, T. C. Clancy, R. McGwier, R. Tandon, S. Sodagari, and J. H. Reed. PHY-layer resiliency in OFDM communications: A tutorial. *IEEE Communications Surveys & Tutorials*, 17(1):292–314, 2015.

[37] I. Siomina and D. Yuan. Load balancing in heterogeneous LTE: Range optimization via cell offset and load-coupling characterization. In *Communications (ICC), 2012 IEEE International Conference on*, pages 1357–1361. IEEE, 2012.

[38] I. Siomina and D. Yuan. Optimizing small-cell range in heterogeneous and load-coupled LTE networks. *IEEE Transactions on Vehicular Technology*, 64(5):2169–2174, 2015.

[39] S. Tekinay. *Next generation wireless networks*, volume 598. Springer Science & Business Media, 2006.

[40] H. Thapliyal, V. Khalus, and C. Labrado. Stress detection and management: A survey of wearable smart health devices. *IEEE Consumer Electronics Magazine*, 6(4):64–69, Oct 2017.

[41] J. Wang and R. Rouil. Assessing coverage and throughput for d2d communication. In *2018 IEEE International Conference on Communications (ICC)*, pages 1–6, May 2018.

[42] Q. Wang, W. Wang, S. Jin, H. Zhu, and N. T. Zhang. Smart media pricing (smp): Non-uniform packet pricing game for wireless multimedia communications. In *2016 IEEE Conference on Computer Communications Workshops (INFOCOM WKSHPS)*, pages 27–32, April 2016.

[43] W. Wang and Q. Wang. Price the QoE, not the data: SMP-economic resource allocation in wireless multimedia Internet of Things. *IEEE Communications Magazine*, 56(9):74–79, Sept 2018.

[44] W. Wang, Q. Wang, and K. Sohraby. Multimedia sensing as a service (msaas): Exploring resource saving potentials of at cloud-edge iot and fogs. *IEEE Internet of Things Journal*, 4(2):487–495, April 2017.

[45] Y.-C. Wang and C.-A. Chuang. Efficient eNB deployment strategy for heterogeneous cells in 4G LTE systems. *Computer Networks*, 79:297–312, 2015.

[46] W. H. Wong, J. K. Ng, and W. M. Yeung. Wireless LAN positioning with mobile devices in a library environment. In *Distributed Computing Systems Workshops, 2005. 25th IEEE International Conference on*, pages 633–636. IEEE, 2005.

[47] S. Wu, J. B. Rendall, M. J. Smith, S. Zhu, J. Xu, H. Wang, Q. Yang, and P. Qin. Survey on prediction algorithms in smart homes. *IEEE Internet of Things Journal*, 4(3):636–644, June 2017.

[48] Y. Wu, W. Yu, D. Griffith, and N. Golmie. A dynamic rate adaptation scheme for M2M communications. In *Communications (ICC), 2018 IEEE International Conference on*. IEEE, 2018.

[49] Y. Wu, W. Yu, D. W. Griffith, and N. Golmie. Modeling and performance assessment of dynamic rate adaptation for m2m communications. *IEEE Transactions on Network Science and Engineering*, pages 1–1, 2018.

[50] Y. Wu, W. Yu, F. Yuan, J. Zhang, C. Lu, J. Nguyen, and D. Ku. A cross-domain optimization scheme for manet communications in heterogeneous networks. *EAI Endorsed Transactions on Wireless Spectrum*, 3(12), 12 2017.

[51] H. Xu, W. Yu, D. Griffith, and N. Golmie. A survey on industrial internet of things: A cyber-physical systems perspective. *IEEE Access*, pages 1–1, 2018.

[52] H. Xu, W. Yu, A. Hematian, D. Griffith, and N. Golmie. Performance evaluation of energy efficiency with sleep mode in ultra dense networks. In *2018 International Conference on Computing, Networking and Communications (ICNC)*, pages 747–751, March 2018.

[53] W. Yu, F. Liang, X. He, W. G. Hatcher, C. Lu, J. Lin, and X. Yang. A survey on the edge computing for the internet of things. *IEEE Access*, 6:6900–6919, 2018.

[54] W. Yu, H. Xu, A. Hematian, D. Griffith, and N. Golmie. Towards energy efficiency in ultra dense networks. In *2016 IEEE 35th International Performance Computing and Communications Conference (IPCCC)*, pages 1–8, Dec 2016.

[55] W. Yu, H. Xu, J. Nguyen, E. Blasch, A. Hematian, and W. Gao. Survey of public safety communications: User-side and network-side solutions and future directions. *IEEE Access*, pages 1–1, 2018.

[56] W. Yu, H. Xu, H. Zhang, D. Griffith, and N. Golmie. Ultra-Dense Networks: Survey of state of the art and future directions. In *Proc. of IEEE 25th International Conference on Computer Communication and Networks (ICCCN)*, 2016.

[57] W. Yu, H. Zhang, Y. Wu, D. Griffith, and N. Golmie. A framework to enable multiple coexisting internet of things applications. In *2018 International Conference on Computing, Networking and Communications (ICNC)*, pages 637–641, March 2018.

[58] J. Zhang, C. Lu, and W. Yu. Towards lte/lte-a bandwidth efficiency in internet-of-things. In *Proc. of IEEE/ACIS International Conference on Computer and Information Science (ICIS)*, June 2019.